

Silicon nanowire electromechanical switches for logic device application

Qiliang Li¹, Sang-Mo Koo², Monica D Edelstein¹, John S Suehle¹
and Curt A Richter¹

¹ Semiconductor Electronics Division, National Institute of Standards and Technology (NIST),
100 Bureau Drive, Gaithersburg, MD 20899, USA

² Department of Electronic Materials Engineering, Kwangwoon University, Seoul 139-701,
Korea

E-mail: Qiliang.Li@nist.gov and Curt.Richter@nist.gov

Received 1 March 2007, in final form 7 June 2007

Published 6 July 2007

Online at stacks.iop.org/Nano/18/315202

Abstract

We report the fabrication and characterization of nanowire electromechanical switches consisting of chemical-vapour-deposition-grown silicon nanowires suspended over metal electrodes. The devices operate as transistors with the suspended part of the nanowire bent to touch metal electrodes via electromechanical force by applying voltage. The reversible switching, large on/off current ratio, small subthreshold slope and low switching energy compared to current CMOSFET make the switches very attractive for logic device application. In addition, we have developed a physical model to investigate the switching characteristics and extract the material properties.

(Some figures in this article are in colour only in the electronic version)

1. Introduction

During the past three decades of great success, silicon complementary metal–oxide–semiconductor field effect transistors (CMOS FET) have been aggressively scaled down to achieve better performance and lower power consumption. Beyond the CMOS scaling, which will become more difficult in the future, next-generation logic devices require alternative strategies, such as resonant tunnelling devices, single-electron transistors, molecular and spin devices [1–5]. However, the operation of these devices still represents a charge-based mechanism with the similar thermodynamic limit as CMOS. New technologies based on something different than electronic charge, such as nano-electromechanical systems (NEMS) and optical computing, may extend the functionalities and open up exponential opportunities for future electronic circuitry [1]. We have previously reported the fabrication of a simple NEMS test structure consisting of a Si nanowire (SiNW) suspended over metal electrodes [6]. In this paper, we demonstrate the integration and characterization of 2-terminal (2-T) and 3-terminal (3-T) electromechanical switches (EMSs). These switches are turned on/off via electromechanical force by applying a voltage between a SiNW suspended as a cantilever and the bottom metal electrodes. The switching of the EMS, which can be

operated as a field effect transistor, depends on the nanowire material's mechanical properties and the device geometry. The reversible switching, small subthreshold slope, low switching energy and large on/off ratio indicated that the SiNW EMS is very attractive for logic applications. In addition, we have developed a model to investigate the physics of the electromechanical switching and mechanical properties of nanowires. It should be noted that nanowire NEMS has been used to investigate the mechanical properties of nanowires and nanotubes [7, 8], and NEMS switches have been fabricated with carbon nanotubes by using e-beam lithography [9]. A suspended SiNW switching system used in this study may provide an alternative and perhaps simpler strategy for achieving electromechanical switching and characterizing the material properties of chemically grown nanowires.

2. Fabrication of electromechanical switches

The SiNWs used in this study (figure 1(a)) were prepared by using low-pressure chemical vapour deposition (LPCVD) under 500 mTorr SiH₄, at 450 °C, with thin Au films (~2 nm) as the catalyst via a vapour–liquid–solid mechanism [10, 11]. Nanowires of 20–300 nm in diameter and 2–150 μm in length were obtained. From transmission electron microscopy (TEM)

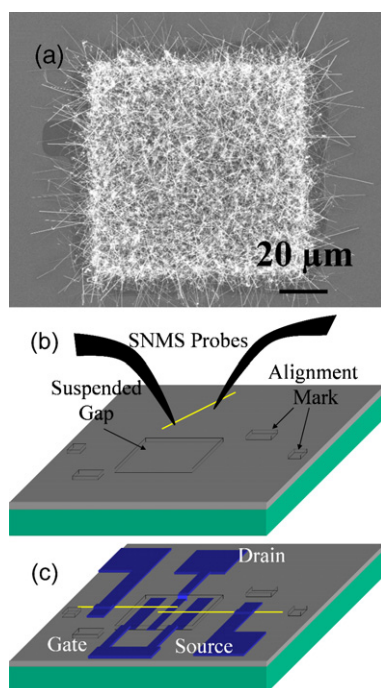


Figure 1. (a) SEM image of Si nanowires grown from the patterned Au catalyst on SiO₂/Si. (b) A SiNW was picked up and transferred to the predefined location of a device substrate by the single nanowire manipulation system probes. (c) The SiNW was patterned with metal contacts (e.g. 3-T EMS has source, drain and gate contacts.) by compatible photolithographic processes.

characterization (data not shown), the SiNWs with a hexagonal cross section grow along the expected [111] direction [12] with a spacing between the (111) planes, which are oriented perpendicular to the SiNW growth direction ≈ 0.31 nm as determined from TEM images.

As shown in the schematic drawing (figures 1(b) and (c)), the nanowire cantilever switches were formed by manipulating SiNWs to align them onto a device substrate by using a single nanowire manipulation system (SNMS) [6] and compatible fabrication processes. First, the SiNWs were removed into a suspension of DI water by sonication (1 min). The SiNW solution was dispersed onto a template substrate and dried for 4 h under vacuum at 100 mTorr. The SiNWs were then manipulated and placed in predefined locations on a device substrate by using a lab-made SNMS so that one side of the SiNWs lies on a thicker oxide (~ 600 nm in thickness) and the other side is suspended over a metal electrode (for 2-T EMS) or a thinner oxide (~ 200 nm in thickness) (for 3-T EMS) (see figure 1(b)). Two kinds of switches (2- and 3-T switches) were prepared in this study by using slightly different processes. For the fabrication of 2-T EMSs, the suspended gap was obtained by dry-etching 400 nm of the 600 nm thermal SiO₂ followed by Au/Al (10 nm/10 nm) deposition and lift-off to form the bottom electrode of the switch. After the alignment of a SiNW (110 nm in diameter) with SNMS, a second-level metal (20 nm/60 nm of Au/Al) was patterned onto the part of the SiNW lying on the 600 nm oxide to clamp the nanowire in place and form the top electrode. For the fabrication of 3-T EMSs, the suspending gap was obtained by dry-etching 400 nm of the 600 nm thermal SiO₂. After the manipulation

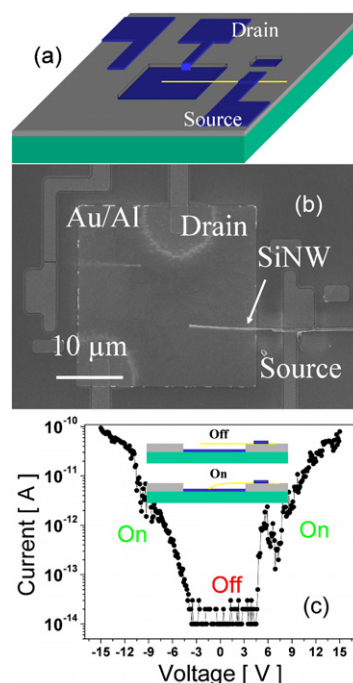


Figure 2. (a) Schematic of a 2-T EMS; (b) SEM image of a 2-T EMS; (c) the typical switching current–voltage characteristics of the 2-T EMS with an inset showing the switch on/off diagram.

and alignment of SiNWs to the designed locations, the bottom electrodes (drain and gate) and top electrode (source) were formed in a single step (see figure 1(c)). All the metal patterns were obtained by using regular photolithographic and metal lift-off processes with an Au layer on the top of the Al layer.

3. Characterization of electromechanical switches

In this work, we have prepared 2-T and 3-T EMSs acting similarly as a current switch and transistor, respectively. A schematic drawing and SEM images of a 2-T switch are shown in figures 2(a) and (b), respectively. The bottom and top electrodes are assigned as the drain and source of the 2-T EMS as shown in the images. The typical switching current–voltage characteristics of a 2-T EMS are shown in figure 2(c) with an inset schematically showing a switch on/off diagram. The 2-T EMS stays off until the applied voltage between the source and drain electrodes is raised above the threshold voltage, V_t ($V_t = 3.8$ V for the example shown in figure 2(c)) and a significant increase in current is observed. During the operation, the suspended part of the SiNW was bent down to touch the bottom electrode by the electromechanical force as it reached a snap-down point at V_t . The on/off ratio of current measured at 9 and 3.8 V is about 10^3 . Such reversible current–voltage switching is observed at both negative and positive applied voltages.

This 2-T EMS is a very simple structure and an efficient switch; however, it has two disadvantages which limit its applications. First, the on-state current is relatively low due to the high contact resistance between the intrinsically doped semiconducting SiNW and the bottom metal electrode. Second, it cannot be operated as a gate-controlled transistor

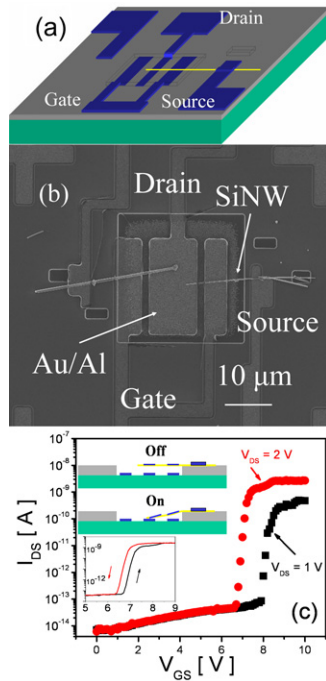


Figure 3. (a) Schematic of a 3-T EMS; (b) SEM image of two 3-T EMSs; (c) the typical switching current–voltage characteristics of the 3-T EMS in the right side of the SEM image. The top inset shows the switch on/off diagram and the bottom inset shows the hysteresis of $I_{DS}-V_{GS}$ as the gate voltage is swept from $V_{GS} = 0$ to 9.0 V and then back to 0 V at $V_{DS} = 2.0$ V.

with gain. To solve these problems, we have fabricated a 3-T EMS with self-aligned source, drain and gate electrodes. The schematic of a 3-T EMS is shown in figure 3(a). After the manipulation and alignment of SiNWs to the designed locations, the bottom electrodes (drain and gate) and top electrode (source) were formed in a single step. This differs from the fabrication of 2-T EMSs which have the bottom electrode formed before the SiNW alignment. The same types of metals have been deposited for both the 2-T EMSs and 3-T EMSs. However, during the fabrication of the 3-T EMS electrodes, the metals are also deposited on the suspended nanowires. This metal directly deposited on the SiNW is expected to lower (i.e. improve) the contact resistance between the SiNW and the bottom drain electrode when the switch is closed. The two bottom electrodes and the top electrode were assigned as the drain, gate and source of the switch as shown in figure 3(a). During the operation of a 3-T EMS, the gate voltage is controlled independently of the drain voltage, which is similar to a conventional MOSFET.

A SEM image of a 3-T EMS is shown in figure 3(b) with the assigned electrodes. Figure 3(c) shows typical switching current–voltage characteristics of a 3-T EMS with the top inset schematically illustrating the on/off configurations. As the gate to source voltage (V_{GS}) increases with a constant drain to source voltage (V_{DS}), the electrostatic force applied to the SiNW increases and bends the wire down to the bottom electrodes. As the suspended end of the SiNW touches the drain electrode at a threshold voltage (e.g. $V_t = 7.9$ V at $V_{DS} = 1.0$ V for the device shown in figure 3(c)), the drain–source current (I_{DS}) is turned on. Since the gate electrode is

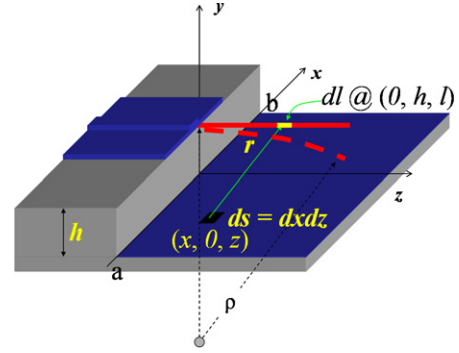


Figure 4. Schematic of a suspending SiNW over a metal electrode with the suspended height h , length L , radius of bending curvature ρ and the charge of unit area at $(x, 0, z)$ on the bottom electrode applying a force on the SiNW at $(0, h, l)$.

closer than the drain electrode to the source electrode in the set-up, the SiNW bends over the gate electrode, with it initially touching the drain to close the switch. As shown in the bottom inset of figure 3(c), an $I_{DS}-V_{DS}$ hysteresis is observed when the gate voltage is scanned from $V_{GS} = 0$ to 9.0 V (which is above V_t) then back to 0 V. This hysteresis arises from the surface electrostatic force between the SiNW and the drain electrode surface. In the 3-T configuration, V_t is determined by the electrostatics between the nanowire and both the gate and drain electrodes. A higher V_{DS} leads to a smaller V_t due to the larger total attractive force associated with the drain electrode in combination with the gate electrode. Compared to the V_t of a 2-T EMS, a much higher V_{GS} is needed in order to pull the SiNW down in contact with the gate electrode in a 3-T EMS due to the much smaller gate electrode area. The 3-T EMS has an on/off current gain of $\sim 10^4$ and a subthreshold slope of ~ 75 mV/dec at a $V_{DS} = 1.0$ V if it is considered as a conventional field effect transistor. The improved lower contact resistance between the metal-coated SiNW and drain of the 3-T EMS leads to a higher on-current and the larger observed on/off ratio when compared with 2-T EMSs. The subthreshold slope and current on/off gain can be further improved by replacing the SiNWs with metallic nanowires.

4. Physical model of electromechanical switches

The threshold voltage for these EMS to ‘close’ the switch and turn on the current is determined by the exact geometry of the SiNW and its mechanical properties (e.g. Young’s modulus: E). When the maximum moment due to electrostatic force (M_e) is greater than the bending moment (M_m) of the SiNW, the SiNW will be bent down into contact with the bottom electrode: the EMS will be closed. A simple estimate of V_t can be made by assuming the initial ‘snap-down’ of the SiNW occurs when $M_e = M_m$. We illustrate this estimation here for the example of a SiNW with a cylindrical geometry with diameter (R), suspending length (L) and suspending height (h). These parameters are shown in the schematic diagram of a suspending SiNW over metal electrode (figure 4).

The potential of the system is [13]

$$\psi(x, y) = \lambda/4\pi\epsilon_0 \ln[x^2 + (y+h)^2/x^2 + (y-h)^2], \quad (1)$$

where λ is the charge density per unit length of the suspended SiNW, ϵ_0 is the permittivity of vacuum, and x , y and z are the coordinates shown in figure 4.

The surface charge density $\sigma(x)$ of bottom electrode is therefore

$$\sigma(x) = - \left[\frac{\partial \psi}{\partial y} \right]_{y=0} \epsilon_0 = CV_t h / \pi L (x^2 + h^2). \quad (2)$$

The electrostatic force between ∂l of the Si nanowire and $\partial x \partial z$ of the bottom electrode can be expressed as

$$\partial F = Q_1 Q_2 / 4\pi \epsilon_0 r^2,$$

where Q_1 and Q_2 are the charges in the differential bottom electrode surface $\partial x \partial z$ and the charges in ∂l of the Si nanowire at $(0, h, l)$; and r is the distance from the bottom surface point $(x, 0, z)$ to the Si nanowire at point $(0, h, l)$: $r^2 = x^2 + h^2 + (z - l)^2$. The direction of ∂F is in the r direction. We have

$$Q_1 = \sigma(x) \partial x \partial z$$

$$Q_2 = CV_t \partial l / L.$$

The electrostatic force applied on the Si nanowire at $(0, h, l)$ by the charges in the bottom electrode surface $\partial x \partial z$ at the perpendicular direction (∂F_{\perp}) is therefore

$$\partial F_{\perp} = \partial F h / r = \sigma(x) CV_t h \partial x \partial z \partial l / 4\pi \epsilon_0 r^3 L. \quad (3)$$

So the electrostatic moment on the Si nanowire at point $(0, h, l)$ due to ∂F_{\perp} is

$$\partial M_e = l \partial F_{\perp} = \sigma(x) CV_t h l \partial x \partial z \partial l / 4\pi \epsilon_0 r^3. \quad (4)$$

The maximum moment due to electrostatic force (M_e) is therefore

$$M_e \approx (C^2 V_t^2 h / 4\pi^2 \epsilon_0 L^2) In, \quad (5)$$

where the unitless integration term In is

$$In = \int_a^b \int_0^L \int_0^L \partial x \partial z \partial l h l / (x^2 + h^2) \times [x^2 + h^2 + (z - l)^2]^{3/2}. \quad (6)$$

a and b are $-10 \mu\text{m}$ and $15 \mu\text{m}$, respectively, representing the distance from the SiNW to the left and right edges of the bottom electrodes as shown in figure 3. In is numerically calculated as 467 for this specific geometry. In decreases dramatically as a and b increase to $1 \mu\text{m}$. For a SiNW with a cylindrical cross section suspended over a metal surface the capacitance, C , of the system is [13]

$$C \approx 2\pi \epsilon_0 L / \cosh^{-1}(2h/R), \quad (7)$$

which is a slight over-estimation for a SiNW over a semi-finite or large finite metal surface. For the geometry here, C is calculated as $\approx 2.0 \times 10^{-16}$ F. A more detailed theoretical study of C for a similar suspended nanowire system has been reported [17], and more precise calculations of C based on special nanowire geometries [14] and the electric field effect [15] have been reported.

With $M_m = EI/\rho$ [16], the Young's modulus E , V_t and switching energy (ΔW_S) are expressed as the following:

$$E \approx (C^2 V_t^2 h \rho / 4\pi^2 \epsilon_0 L^2 I) In; \quad (8)$$

$$V_t \approx \sqrt{4\pi^2 \epsilon_0 L^2 EI / In C^2 h \rho}; \quad (9)$$

$$\Delta W_S = \frac{1}{2} C V_t^2 = 2\pi^2 \epsilon_0 L^2 EI / Ch \rho In; \quad (10)$$

where I is the moment of inertia of the SiNW, ρ is the radius of curvature and EI is the flexural rigidity of the SiNW [16]. ρ can be expressed as $\rho = (h^2 + L^2)/2h$. Assuming the SiNW has a cylindrical cross section, I can be calculated as $I = \frac{\pi}{64} \times R^4$. Thus, for the example shown in figure 2, E of a cylindrical SiNW extracted by this method is ≈ 118 GPa, which is within the range of the reported values [18].

C , V_t and switching energy strongly depend upon the details of the bottom electrode geometry. It should be noted that the accuracy of the Young's modulus extracted by this simple estimation also depends on how well the equations represent the specific geometry of the SiNWs and the electrode. For example, for a SiNW with a hexagonal cross section (which more closely represents the SiNWs grown in the [111] direction [14] than the cylindrical example) with a side length, $w = \frac{1}{2}R$, the capacitance is calculated as $\approx 1.87 \times 10^{-16}$ F by following the reported approach [14]. The moment of inertia is $I = \frac{5\sqrt{3}}{256} \times R^4$. For this example, of the SiNW with a hexagonal cross section, the E (proportional to C^2/I) is calculated as 150 GPa. Thus, the estimated Young's modulus is different by $\approx 24\%$ for these two different geometries. In addition, the electric field will also affect the accuracy of the extracted Young's modulus [15]. The switching energy of the 2-T EMS shown in figure 2 is about 2.0×10^{-14} J. Theoretically, with $E = 107$ GPa (for the bulk Si), $L = 1 \mu\text{m}$, $R = 10$ nm and $h = 10$ nm, the switching energy is as low as 3.7×10^{-19} J. In addition, based on the developed model and equation (9), ideally the device operation is unaffected by the temperature and the subthreshold slope has no limit. While there are many subtleties associated with using this technique to derive the accurate value of the Young's modulus, it can be used to precisely compare relative changes in E for nanowires with different structural properties (such as a change in the radius for nanowires of a known material or a comparison of nanowires with the same diameter formed from different materials).

5. Conclusions

In summary, we have fabricated 2-T and 3-T electromechanical switches consisting of suspended nanowires over metal electrodes. We have shown that the EMS devices are attractive for the following reasons. (1) The devices have no power consumption in the off-state and very small switching energy ($\sim 10^{-14}$ J). Virtually no current passes through the switch until the SiNW is mechanically 'bent' and brought into contact with the bottom electrode and a large on-current is observed. (2) The devices have small subthreshold slope (~ 75 mV/dec). Theoretically, the switch with more conductive nanowire (e.g. metal nanowires) will have a much smaller subthreshold slope than that of CMOS FET (i.e. ~ 60 mV/dec) [19]. (3) The switches are turned on/off reversibly with large on/off current gain ($\sim 10^4$). (4) The devices will not be affected by the temperature as the CMOS FETs.

Acknowledgments

Contribution of the National Institute of Standards and Technology is not subject to US copyright. The authors are grateful to the support of the NIST Office of Microelectronics Programs and NIST Semiconductor Electronics Division.

References

- [1] ITRS 2005 *Emerging Research Devices*
- [2] Chen R H, Korotkov A N and Likharev K K 1996 *Appl. Phys. Lett.* **68** 1954
- [3] Fay P, Jiang L, Xu Y, Bernstein G H, Chow D H, Schulman J N, Dunlap H L and De Los Santos H J 2001 *IEEE Trans. Electron Devices* **48** 1282
- [4] Nikonov D E and Bourianoff G I 2005 *IEEE Trans. Nanotechnol.* **4** 206
- [5] Seminario J M, Derosa P A, Cordova L E and Bozard B H 2004 *IEEE Trans. Nanotechnol.* **3** 215
- [6] Li Q, Koo S-M, Richter C A, Edelstein M D, Bonevich J E, Kopanski J J, Suehle J S and Vogel E M 2007 *IEEE Trans. Nanotechnol.* **6** 256
- [7] Wang Z L, Dai Z R, Gao R P and Gole J L 2002 *J. Electron. Microsc.* **51** S79
- [8] Wong E W, Sheehan P E and Lieber C M 1997 *Science* **277** 1971
- [9] Jang J E, Cha S N, Choi Y, Amaratunga G A J, Kang D J, Hasko D G, Jung J E and Kim J M 2005 *Appl. Phys. Lett.* **87** 163114
- [10] Wagner R S and Ellis W C 1964 *Appl. Phys. Lett.* **4** 89
- [11] Givargizov E I 1975 *J. Cryst. Growth* **31** 20
- [12] Morales A and Lieber C 1998 *Science* **279** 208
- [13] Morse P M and Feshbach H 1953 *Methods of Theoretical Physics* vol 2 (New York: McGraw-Hill)
- [14] Wunnicke O 2006 *Appl. Phys. Lett.* **89** 083102
- [15] Zheng X J and Zhu L L 2006 *Appl. Phys. Lett.* **89** 153110
- [16] Gere J M and Timoshenko S P 1991 *Mechanics of Materials* 3rd edn (Boston, MA: PWS-Kent)
- [17] Tang Z, Xu Y, Li G and Aluru N R 2005 *J. Appl. Phys.* **97** 114304
- [18] Menon M, Srivastava D, Ponomareva I and Chernozatonskii L A 2004 *Phys. Rev. B* **70** 125313
- [19] Taur T and Ning T H 1998 *Fundamentals of Modern VLSI Devices* (New York: Cambridge University Press)